Microstructures and Dielectric Properties of the Ferroelectric Fluoropolymers Synthesized via Reductive Dechlorination of Poly(vinylidene fluoride-*co*-chlorotrifluoroethylene)s

Yingying Lu,[†] Jason Claude,[†] Qiming Zhang,[†,‡] and Qing Wang*[,†]

Department of Materials Science and Engineering, and Department of Electrical Engineering, The Pennsylvania State University, University Park, Pennsylvania 16802

Received June 12, 2006; Revised Manuscript Received July 26, 2006

ABSTRACT: Ferroelectric fluoropolymers containing vinylidene fluoride (VDF), trifluoroethylene (TrFE), and chlorotrifluoroethylene (CTFE) have been prepared over a wide composition range by a two-step approach consisting of copolymerization of VDF and CTFE and a subsequent reductive dechlorination reaction. Due to the similar reactive ratios between VDF and CTFE and quantitative dechlorination yields, the chemical structures and compositions of the resulting terpolymers can be precisely controlled. The structural characteristics including microstructure, chain conformation, and crystallinity of the polymers have been carefully elucidated as a function of the chemical composition by ^{1}H and ^{19}F NMR, Fourier transform infrared spectroscopy, and wide-angle X-ray diffraction. The influence of the polymer compositions on thermal transitions and dielectric constants has also been investigated. A Curie temperature of 23 °C and dielectric constant of 50 measured at ambient temperature and 1 kHz have been achieved at the terpolymer composition of 78.8 mol % VDF, 14 mol % CTFE, and 7.2 mol % TrFE.

Introduction

Poly(vinylidene fluoride) (PVDF) based ferroelectric polymers have been the subject of intense research since the discovery of piezoelectricity in PVDF by Kawai et al. in 1969.[1,2] Part of the motivation for these research efforts is the wide variety of applications of these materials in advanced electromechanical devices such as transducers, actuators, artificial muscles, sensors, and microfluidic systems.[3] It has been shown that the copolymers of vinylidene fluoride (VDF) and trifluoroethylene (TrFE), P(VDF−TrFE)s, exhibit excellent piezoelectric sensitivity for the stress and strain sensing.[4] For example, the piezoelectric coefficient g_{33} for P(VDF−TrFE)s is 0.24 V m/N, which is 2 orders of magnitude greater than that of PZT (the most widely used piezoceramic sensor material) with a g_{33} of 0.0023 Vm/N.[5] Nevertheless, these polymers exhibit a Curie transition from ferroelectric to paraelectric (F−P) phases at temperatures much higher than room temperature. At the Curie transition, the dielectric constant of the copolymer reaches a maximum due to the increase in mobility of the C−F dipoles. The lowest Curie temperature observed is about 70 °C for the P(VDF−TrFE) with 45 mol % TrFE.[6] Consequently, the dielectric responses of the C−F dipoles in P(VDF−TrFE) copolymers to the electric field is rather weak at ambient temperature, as revealed by a relatively low dielectric constant (∼14).[7]

Recently, several promising approaches have been developed to reduce the size of the crystalline domain in P(VDF−TrFE)s as a way of increasing the dielectric response. These methods include electron irradiation,[8] mechanical deformation,[9] chemical cross-linking and blending,[10] and crystallization at various conditions.[11] It is envisaged that the small ferroelectric domains are more easily oriented by an applied field, leading to a reduced energy barrier in the F−P phase transition and large dielectric responses at ambient conditions. Indeed, the P(VDF−TrFE) copolymers treated by high-energy electron irradiation exhibit orders of magnitude improvement in elastic energy density (>1 J/cm^3) and electrostrictive strain (>5%).[8a] It has been established that the defects introduced by irradiation break up the macroscopic polar regions into nanoscopic domains and convert the polymer from a normal ferroelectric state to a ferroelectric relaxor.[12] As a result, the electron beam irradiated P(VDF−TrFE)s show a slim polarization loop and a very high dielectric constant at room temperature. Similar results have been obtained in PVDF−based terpolymers, poly(vinylidene fluoride-*co*-trifluoroethylene-*co*-chlorotrifluoroethylene)s P(VDF−TrFE−CTFE)s, in which the bulky chlorotrifluoroethylene (CTFE) components in the terpolymer function as random defects to reduce crystal size.[13] The high dielectric constants in these polymers are attractive for applications in electrical energy storage such as stationary power generation and miniature capacitors for portable electronics and electric vehicles.[14] High dielectric constant polymers also hold great potential as nonvolatile memory elements and gate dielectrics with low operational voltages for applications in integrated flexible logic circuits, flat panel devices, and sensor arrays.[15]

The ferroelectric P(VDF−TrFE-CTFE) terpolymers are generally produced by free-radical polymerization of the three monomers using emulsion, suspension, and solution methods.[13,16] Unfortunately, due to the large difference in the reactivity between TrFE and other two comonomers, e.g. r_1(TrFE) = 0.5 and r_2(VDF) = 0.7,[17] access to these polymers is often challenged by factors such as inhomogeneous composition distribution, significantly varied dielectric properties depending on polymerization method and conversion, and the limited numbers of the polymers available for structure−property correlation study. Overcoming these restraints, which have prevented the ferroelectric fluoropolymers from reaching their full potential, requires development of new polymerization strategies. More recently, we presented a new synthetic approach

* To whom correspondence should be addressed. E-mail: wang@matse.psu.edu.
[†] Department of Materials Science and Engineering.
[‡] Department of Electrical Engineering.

10.1021/ma061311i CCC: $33.50
Published on Web 09/07/2006

Scheme 1. Synthesis of the Ferroelectric P(VDF−CTFE−TrFE) Terpolymers

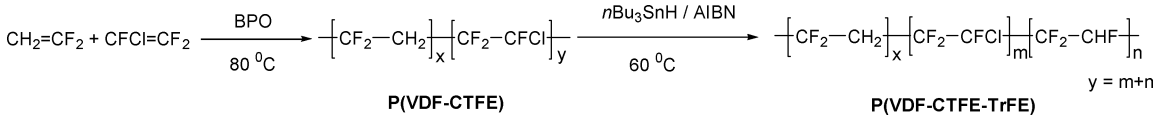

toward the ferroelectric terpolymers exhibiting high dielectric constants and low loss tangents at ambient temperature.[18] In this paper, we describe the detailed studies on the synthesis and structural characterization of a library of the ferroelectric terpolymers composed of VDF, TrFE, and CTFE. The microstructure, chain conformation, and thermal and dielectric properties have been investigated as a function of the polymer composition.

Experimental Section

Materials. Unless otherwise noted, all solvents and reagents were purchased from Aldrich and used as received. All manipulations of gas-condense transfer were carried out with rigorous exclusion of oxygen and moisture on a dual-manifold Schlenk line with 10^{-6} Torr high vacuum. Benzoyl peroxide (BPO) was purchased from Aldrich and purified by recrystallization from methanol and acetone. Tetrahydrofuran (THF) was distilled from sodium benzophenone ketyl under nitrogen. Vinylidene fluoride and chlorotrifluoroethylene were purchased from SynQuest Laboratory Inc. and purified by a freeze−thaw process prior to use.

Preparation of P(VDF−CTFE)s. A stainless steel vessel equipped with a magnetic stir bar was charged with 0.12 g (0.5 mmol) of BPO, and 30 mL of acetonitrile was added. The vessel was sealed, submerged in liquid nitrogen, and degassed on a vacuum line. Then 18.4 g of VDF and 7.3 g of CTFE were added to the reactor at liquid nitrogen temperature. The vessel was warmed to ambient temperature and heated for 6 h at 80 °C. After this time, the volatiles were vented, and subsequent precipitation into methanol, washing by hexane, and drying in vacuo, afforded 9.4 g of a white solid identified as P(VDF−CTFE). ^{1}H NMR (DMSO-d_6, ppm): δ 8.1 (d, 2H, *o*-C_6H_5), 7.7 (t, 1H, *p*-C_6H_5), 7.5 (t, 2H, *m*-C_6H_5), 2.6−3.6 (m, 2H, $-CF_2CH_2CF_2-$, head-to-tail structure of VDF segment), 2.2−2.5 (m, 2H, $-CF_2CH_2CH_2CF_2-$, tail-to-tail structure of VDF segment).

Preparation of P(VDF−CTFE−TrFE)s. To a 50-mL round-bottom flask was added P(VDF−CTFE) copolymers (0.8 g), AIBN (42.8 mg, 0.25 mmol), and THF (20 mL). The reaction solution was bubbled with argon for 20 min and was followed by freeze−pump−thaw cycles and a final argon backfill to provide a positive atmosphere. After the mixture was stirred at 60 °C for 30 min, tri(*n*-butyl)tin hydride (0.14 mL, 0.51 mmol) was added by syringe. The solution was kept stirring at 60 °C for 24 h before it was quenched with methanol. The precipitate was washed with hexane and dried in vacuo to yield 0.7 g of P(VDF−CTFE−TrFE)s as a white solid. Tin byproducts were removed by dissolving the polymers in THF and stirring of the polymer solution with aqueous potassium fluoride. After purification, residual tin byproducts were not found in the polymers by NMR. ^{1}H NMR (DMSO-d_6, ppm): δ 8.1 (d, 2H, *o*-C_6H_5), 7.7 (t, 1H, *p*-C_6H_5), 7.5 (t, 2H, *m*-C_6H_5), 5.3−5.7 (m, 1H, $-CFHCF_2-$ of TrFE segment), 2.6−3.6 (m, 2H, $-CF_2CH_2CF_2-$, head-to-tail structure of VDF segment), 2.2−2.5 (m, 2H, $-CF_2CH_2CH_2CF_2-$, tail-to-tail structure of VDF segment).

Characterization. ^{1}H and ^{19}F NMR spectra were recorded on a Bruker AM-300 spectrometer instrument. Size exclusion chromatography (SEC) was performed in a THF mobile phase with a Waters 1515 isocratic pump. The thermal transition data were obtained by a TA Instruments Q100 differential scanning calorimeter (DSC) at a heating rate of 10 °C/min. Wide-angle X-ray diffraction (WAXD) measurements were conducted using a Scintag diffractometer with Cu Kα radiation. Peak deconvolution was performed using a peak fitting program and Pearson VII peaks. FTIR spectra were recorded on Varian Digilab FTS-800 spectrometer in the temperature range from room temperature to 135 °C. The dielectric constants of the polymers were acquired using a HP multifrequency LCR meter (HP 4284A) at room temperature with a 1 V bias.

Results and Discussion

Synthesis of P(VDF−CTFE)s and P(VDF−CTFE−TrFE)s. The synthetic strategy outlined in Scheme 1 involves the copolymerization of VDF and CTFE using BPO as the initiator followed by a reductive dechlorination reaction to yield the P(VDF−CTFE−TrFE) terpolymer. Since VDF and CTFE possess similar reactivity ratios in free radical polymerization, i.e., $r_1 = 0.70$ (VDF) and $r_2 = 0.72$ (CTFE),[19] the chemical compositions of the P(VDF−CTFE) copolymers are readily controlled by varying the monomer feeding ratios. The resulting P(VDF−CTFE) copolymers then undergo a dechlorination reaction using AIBN as a radical initiator and tri(*n*-butyl)tin hydride as a reduction agent, which reduces the chlorine groups quantitatively and converts CTFE to TrFE.[20] Therefore, by varying the ratio between the reduction reagent and the concentration of CTFE in P(VDF−CTFE) copolymers, the contents of TrFE component in the terpolymers can thus be accurately controlled. A library of 47 P(VDF−CTFE)s and P(VDF−CTFE−TrFE)s with different chemical compositions has been prepared, and the details are tabulated in the Supporting Information. The terpolymers are soluble in common organic solvents, such as THF, DMF, DMSO, methyl ethyl ketone (MEK), etc. GPC measurements in THF, using polystyrene as a standard, indicated a typical number-averaged molecular weight (M_n) of around 60 kDa with a polydispersity of about 1.8.

The compositions of the polymers are determined by ^{1}H and ^{19}F NMR. Figure 1 shows the ^{19}F NMR spectrum of the P(VDF−CTFE) copolymer with a composition of VDF/CTFE = 81.2/18.8 mol %, and the assignments of the peak are listed in Table 1. The chemical compositions of the P(VDF−CTFE)s are calculated according to the integrals of the characteristic peaks of VDF and CTFE in ^{19}F NMR spectra by the following equation:[21]

$$\frac{\text{mol\% VDF}}{\text{mol\% CTFE}} = \frac{I_1 + I_2 + 3I_3 - I_4}{I_5 + I_6 + 2(I_4 - I_3)} \cdot \frac{3}{2}$$

where I_1 is the integral intensity of the resonance area of −92 to −97 ppm, I_2 = −106 to −113.5 ppm, I_3 = −114.3 ppm, I_4= −116.6 ppm, I_5 = −118 to −123.3 ppm, and I_6 = −129.4 to −137.2 ppm. The transformation of the copolymers into the P(VDF−CTFE−TrFE) terpolymers via the dechlorination reaction was confirmed by the appearance of the signals around 5.6 ppm corresponding to the protons from TrFE in the ^{1}H NMR spectra. The molar fraction of TrFE in the terpolymers can be assessed readily by the ratios of the integration values of the distinct peaks centered at 5.6 ppm from TrFE to the signals around 3.1 and 2.3 ppm assigned to the methylene protons of head-to-tail and tail-to-tail sequences of VDF units, respectively.

Polymer Microstructure Studied by NMR. It is found that CTFE is attacked exclusively at its CF_2 carbon by the growing $-CH_2CF_2^{\bullet}$ radical, leading to tail-to-tail placements. As illustrated in the ^{19}F NMR spectrum (Figure 1), the microstructure of the P(VDF−CTFE) copolymer is dominated by the presence

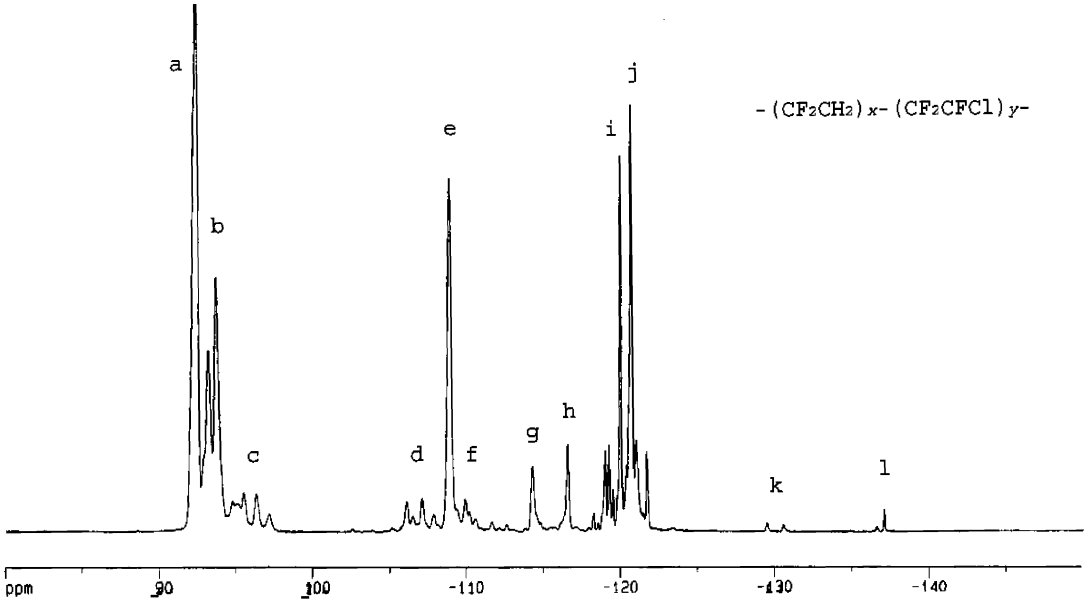

Figure 1. ^{19}F NMR spectrum of the P(VDF−CTFE) copolymer containing 81.2 mol % VDF and 18.8 mol % CTFE.

Table 1. Chemical Shifts and Assignments of ^{19}F NMR Peaks of the P(VDF−CTFE) Copolymer

spectrum range	line	sequence	designation[a]	chemical shift (ppm)	percentage (%)
I_1	a	$-CF_2CH_2CF_2CH_2CF_2-$	VDF−VDF/H−T	−92.36	26.40
	b	$-CFClCH_2CF_2CH_2CF_2-$	CTFE−VDF/T−T	−93.16 to −93.67	19.02
	c	$-CH_2CH_2CF_2CH_2CF_2-$	VDF−VDF−VDF/T−T−H	−94.26 to −97.13	6.203
I_2	d	$-CF_2CFClCF_2CFClCF_2-$	CTFE−CTFE/H−T	−106.05 to −107.82	3.289
	e	$-CF_2CH_2CF_2CF_2CFCl-$	VDF−CTFE/T−T	−108.0 to −109.34	12.78
	f	$-CF_2CFClCF_2CFClCH_2-$	CTFE−CTFE−VDF/H−T−T	−109.34 to −113.10	2.579
I_3	g	$-CF_2CH_2CF_2CF_2CH_2-$	VDF−VDF/T−T	−114.27	2.275
I_4	h	$-CH_2CF_2CF_2CH_2CH_2-$	VDF−VDF/T−T	−116.57	2.336
I_5	i	$-CH_2CF_2CF_2CFClCH_2-$	VDF−CTFE/T−T	−118.25 to −119.98	9.922
	j	$-CF_2CF_2CFClCH_2CF_2-$	CTFE−VDF/T−T	−120.35 to −123.32	10.30
I_6	k	$-CF_2CH_2CFClCF_2CH_2-$	VDF−CTFE−VDF/T−T−H	−129.46 to −130.53	0.238
	l	$-CH_2CF_2CFClCF_2CH_2-$	VDF−CTFE/H−T	−136.57 to −137.17	0.285

[a] The head (H) of the unit is defined as the CF_2 while the tail (T) is defined as the CH_2 or CFCl.

of VDF−VDF head-to-tail ($-CH_2CF_2CH_2CF_2-$) sequence showing around −92.4 ppm (peak a in Figure 1) and VDF−CTFE tail-to-tail ($-CF_2CH_2CClFCF_2-$) structure appearing around −93.4, −108.7, −119.1, and −121.9 ppm (peaks b, e, i, and j in Figure 1). The weak resonance at 126 ppm (peak l in Figure 1) is attributed to a very low content (∼0.285%) of VDF−CTFE head-to-tail ($-CH_2CF_2CFClCF_2-$) sequence, which presumably are the end groups or branching points resulting from the chain-transfer steps involving the chloro monomer units. Consistent with the ^{19}F NMR results, the major peaks showing around 3.1 ppm in the ^{1}H NMR spectra of the copolymers are associated with the methylene protons of head-to-tail VDF−VDF structure. The ^{19}F NMR spectrum of the P(VDF−CTFE−TrFE) terpolymer with a composition of 81.2/7.2/11.6 mol % prepared by reduction of the P(VDF−CTFE) copolymer is illustrated in Figure 2. The chemical shifts and assignments of the peaks observed in the spectrum are summarized in Table 2. The peaks are identified according to the spectra of P(VDF−CTFE)s and the corresponding P(VDF−TrFE) copolymers yielded from complete dechlorination whose details are shown in the Supporting Information.[22] It was found that the main structure of the terpolymer includes VDF−VDF head-to-tail sequence and tail-to-tail sequences of VDF−CTFE and VDF−TrFE ($-CF_2CH_2CClFCF_2-$, $-CF_2CH_2CHFCF_2-$). It is of interest to note that the terpolymers prepared via the reductive route exhibit different microstructures from the ones produced by direct terpolymerization of three comonomers. The ^{19}F NMR spectrum of the terpolymer prepared by terpolymerization and the peak assignments are given in the Supporting Information. VDF−VDF head-to-tail sequences account for 46% of the polymer chains synthesized by direct terpolymerization, while the terpolymer prepared by the reduction reaction contains about 28% VDF−VDF head-to-tail sequences. Beside 6.4% VDF−TrFE tail-to-tail structures, there is about 8.9% VDF−TrFE head-to-tail ($-CH_2CF_2CHFCF_2-$) sequence existing in the terpolymer prepared by direct terpolymerization; this is in marked contrast to the terpolymers generated from reduction reaction, which show no evidence of the existence of VDF−TrFE head-to-tail structures from the ^{19}F NMR measurements. VDF−CTFE exists predominantly as tail-to-tail structures in the both terpolymers. The discrepancy in microstructure leads to significantly different thermal and dielectric properties in these two terpolymers. In general, with the same chemical composition, the terpolymers prepared via direct terpolymerization possess a lower percentage of sequence defects such as head-to-head and tail-to-tail structures in polymer chain, resulting in a higher degree of crystallinity and Curie transition temperature compared to the terpolymers synthesized via the dechlorination reaction.

Chain Conformation Studied by FTIR. As identified in the FTIR measurements, the polymer chain conformation is strongly influenced by the polymer composition. Figure 3 presents the infrared spectra of the terpolymers containing 78.8 mol % VDF, where the absorption bands at 1290 cm^{-1} arise

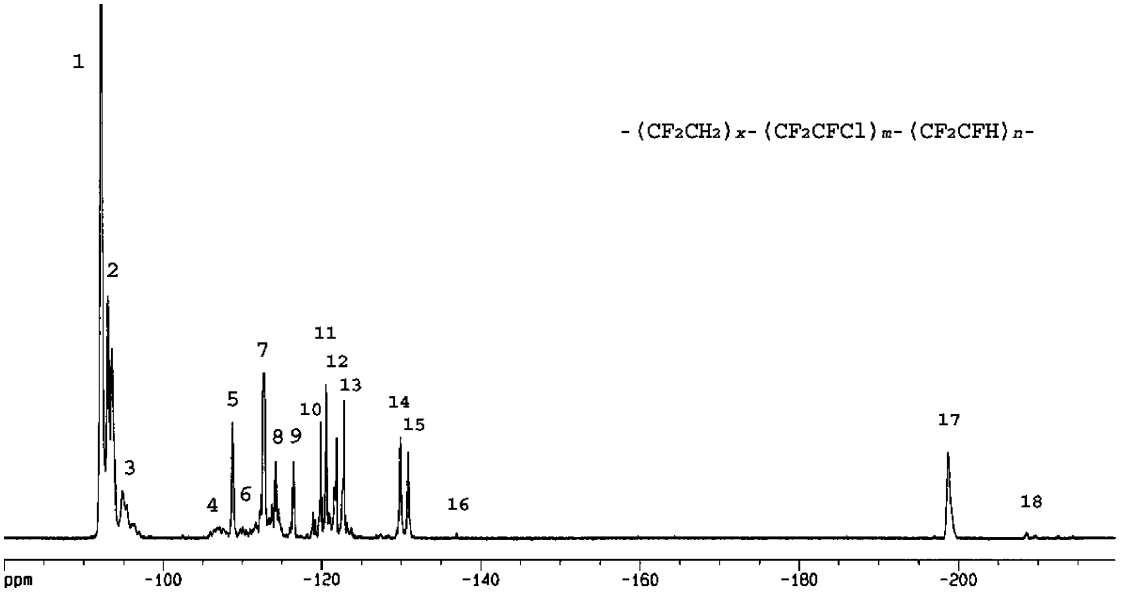

Figure 2. ^{19}F NMR spectrum of the P(VDF−CTFE−TrFE) terpolymer with a composition of 81.2/7.2/11.6 mol %.

Table 2. Assignments of ^{19}F NMR Resonances of the P(VDF−CTFE−TrFE) Terpolymer

peak no.	sequence	designation[a]	chemical shift (ppm)	percentage (%)
1	$-CF_2CH_2CF_2CH_2CF_2-$	VDF−VDF/H−T	−92.36	27.25
2	$-CHFCH_2CF_2CH_2CF_2-$	TrFE−VDF/T−T	−93.16 to −93.63	19.40
	$-CClFCH_2CF_2CH_2CF_2-$	CTFE−VDF/T−T		
3	$-CH_2CH_2CF_2CH_2CF_2-$	VDF−VDF−VDF/T−T−H	−94.35 to −96.46	5.646
4	$-CF_2-CClFCF_2CClFCF_2-$	CTFE−CTFE/H−T	−105.9 to −108.0	1.719
5	$-CF_2CH_2CF_2CF_2CClF-$	VDF−CTFE/T−T	−108.81	3.755
6	$-CF_2CClFCF_2CClFCH_2-$	CTFE−CTFE−VDF/H−T−T	−109 to −112	1.956
7	$-CF_2CH_2CF_2CF_2CHF-$	VDF−TrFE/T−T	−112.68 to −112.84	8.294
8	$-CF_2CH_2CF_2CF_2CH_2-$	VDF−VDF/T−T	−114.21	2.117
9	$-CH_2CF_2CF_2CH_2CH_2-$	VDF−VDF/T−T	−116.52	2.041
10	$-CH_2CF_2CF_2CClFCH_2-$	VDF−CTFE/T−T	−118.96	2.831
11	$-CF_2CF_2CClFCH_2CF_2-$	CTFE−VDF/T−T	−119.81	3.300
12	$-CF_2CHFCF_2CHFCF_2-$	TrFE−TrFE/H−T	−121.68	2.940
13	$-CF_2CHFCF_2CHFCH_2-$	TrFE−TrFE−VDF/H−T−T	−122.79	3.308
14	$-CH_2CF_2CF_2CHFCH_2-$	VDF−TrFE−VDF/T−T	−129.95	2.842
15	$-CF_2CFClCF_2CHFCH_2-$	CTFE−TrFE−VDF/H−T−T	−130.94	2.354
16	$-CH_2CF_2CClFCF_2CH_2-$	VDF−CTFE−VDF/H−T−H	−136.97	0.046
17	$-CF_2CF_2CHFCH_2CF_2-$	TrFE−VDF/T−T	−198.72	5.063
18	$-CH_2CF_2CHFCF_2CH_2-$	VDF−TrFE/H−T	−212.50	0.090

[a] The head (H) of the unit is defined as the CF_2 while the tail (T) is defined as the CH_2 or CFCl.

from the CF_2 stretching vibration of all-trans ($t_{m>4}$) conformation in the β-phase, and the bands at 505 cm^{-1} are attributed to the bending mode of CF_2 in the tttg$^+$tttg$^-$ conformation of the γ-phase.[23] With the increase of TrFE content, the intensities of the absorption band at 1290 cm^{-1} increase, whereas the intensities of the weak absorption bands at 614 cm^{-1} corresponding to the tg$^+$tg$^-$ conformation in the α-phase show little composition dependence. P(VDF−TrFE) copolymers yielded from complete reduction of P(VDF−CTFE)s exhibit largely an all-trans conformation of the β-phase. On the other hand, the peaks corresponding to all-trans conformation are almost absent and the peaks from tttg$^+$tttg$^-$ conformation in the γ-phase become prominent in the P(VDF−CTFE−TrFE) terpolymers containing less than 10 mol % TrFE. This is consistent with those reported earlier by Zhang et al., indicating that the crystalline form of the terpolymers changes from ferroelectric β- to γ-phases upon introduction of bulky CTFE components.[24]

As exemplified in Figure 4, infrared spectra are also examined over a broad temperature range to elucidate the chain conformation. The absorbance at 505, 614, and 1290 cm^{-1} are analyzed to determine the relative fractions of tttg$^+$tttg$^-$, tg$^+$tg$^-$, and all-trans conformations in the polymer, respectively. At room temperature, the polymer with a composition of 81.2 mol % VDF, 7.2 mol % CTFE, and 11.6 mol % TrFE contains

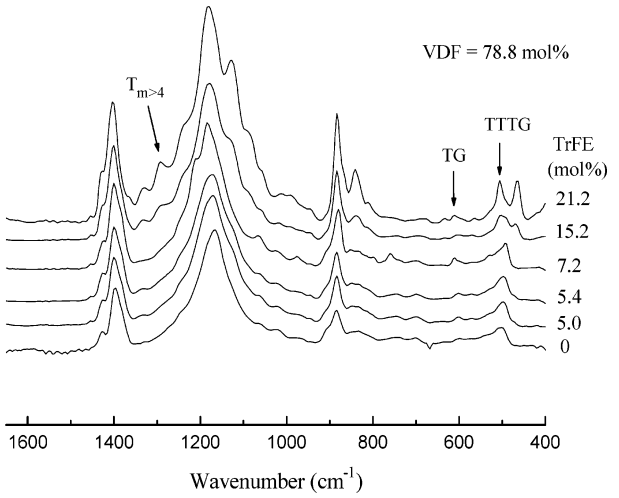

Figure 3. FTIR spectra of the terpolymers containing 78.8 mol % VDF (T_m, all-trans conformation; G, gauche conformation).

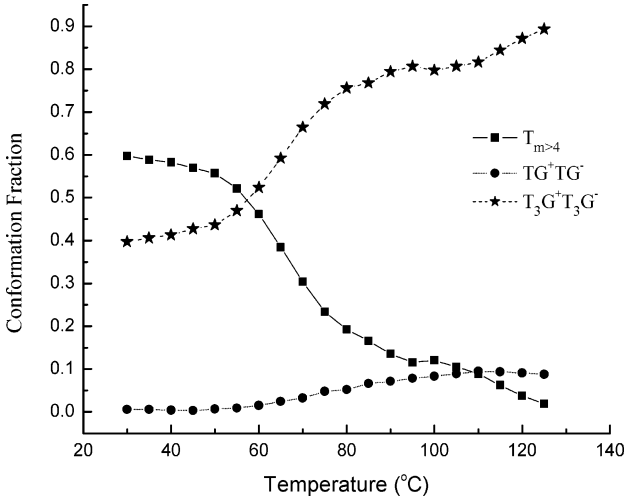

Figure 4. Temperature dependence of the all-trans, $tttg^+tttg^-$, and tg^+tg^- conformation fractions in the P(VDF−CTFE−TrFE) terpolymer with a composition of 81.2/7.2/11.6 mol %.

approximately 60% of the all-trans conformation and 40% of the $tttg^+tttg^-$ sequence. The marked decrease in the all-trans fraction and increase in the $tttg^+tttg^-$ fraction starting around 60 °C is considered to be associated with Curie transition, which roughly matches the endothermic peak at 68 °C observed in the DSC thermogram. Above 120 °C, where the polymer begins to melt, the all-trans structure tends to disappear and the $tttg^+tttg^-$ sequence governs the polymer chains, as expected in the disordered melting state, where the polymer chains rotate freely and favor a laterally expanded, helical conformation.[25] To a large extent, the γ-phase yielded with increasing temperature is at the expense of the ferroelectric β-phase and not of the antipolar α-phase.

Crystalline Structures Studied by WAXD. WAXD is used to investigate the evolution of crystalline structures of the terpolymers with chemical compositions. The WAXD patterns of the terpolymers generally display an unresolved peak at 2θ angle of 18.5° arising from composite (110) and (200) reflections of the ferroelectric phase.[26] The *d*-spacing of these peaks can be computed using Bragg's law, $\lambda = 2d \sin \theta$, where $\lambda = 1.54$ Å. It is assumed that the crystalline geometry is orthorhombic, which has spacing formulas of $\alpha = \beta = \gamma = 90°$ and $1/d_{hkl}^2 = h^2/a^2 + k^2/b^2 + l^2/c^2$. Using the (200) and (110) peaks and above equations, the unit-cell dimensions can be calculated for the terpolymers. The crystallite size is calculated by using Scherrer's formula, $t = \lambda/B \cos \theta$, where *t* is the crystallite size, λ is the wavelength (1.54 Å), *B* is the normalized fwhm (in radians), and θ is the diffraction angle (in radians).[27] The degree of crystallinity can be determined by the ratio of the crystalline peak area to the sum of the areas of the crystalline peaks and the amorphous halo, as fitted from the (200) and (110) peak. The results of lattice spacing (*d*), lattice parameters (*a* and *b*) of the unit cell, crystallite size (*t*), and degree of crystallinity (X_c) are summarized in Table 3. Due to replacement of bulkier chlorine atoms by fluorine, the spacing and volume of the crystal lattice progressively decrease with the increase of TrFE content, which also implies that chlorine atoms are embedded in the unit cells.[24a] Consistent with FTIR results, the degree of crystallinity increases with decreasing CTFE concentration, further confirming that the existence of bulky CTFE components in the terpolymers reduces crystallinity and crystalline size.

Thermal Transitions and Dielectric Properties. As shown in the Supporting Information, the observed relatively sharp melting and Curie phase transitions in DSC studies can be

Table 3. Lattice Constants and Crystallinity of the Terpolymers

polymer composi tion (mol %)			lattice spacing	lattice parameter		crystallite size	degree of crystallinity
VDF	TrFE	CTFE	*d* (nm)	*a*	*b*	*t* (nm)	X_c (%)
73.6	6.4	20.0	4.86	9.72	5.61	15.0	17.7
73.6	12.9	13.5	4.83	9.66	5.58	12.3	32.7
73.6	16.0	10.4	4.77	9.54	5.51	11.2	35.8
73.6	19.7	6.7	4.64	9.28	5.36	11.1	40.4
73.6	26.4	0	4.54	9.08	5.24	11.3	42.4
78.8	5.0	16.2	4.91	9.82	5.67	15.7	28.5
78.8	5.4	15.8	4.92	9.84	5.68	15.6	32.2
78.8	7.2	14.0	4.87	9.74	5.62	13.2	36.3
78.8	15.2	6.0	4.66	9.32	5.38	10.8	42.5
78.8	21.2	0	4.52	9.04	5.22	13.2	50.2
79.2	5.2	15.6	4.91	9.82	5.67	14.8	29.2
79.2	7.2	13.6	4.85	9.70	5.60	14.2	32.9
79.2	9.9	10.9	4.74	9.48	5.47	11.8	33.1
79.2	13.2	7.6	4.65	9.30	5.37	10.7	41.8
79.2	20.8	0	4.47	8.94	5.16	12.2	52.9
81.2	6.7	12.1	4.76	9.52	5.50	15.1	25.3
81.2	7.0	11.8	4.83	9.66	5.58	15.1	32.2
81.2	11.6	7.2	4.53	9.06	5.23	11.4	34.3
81.2	18.8	0	4.43	8.86	5.11	9.62	52.5

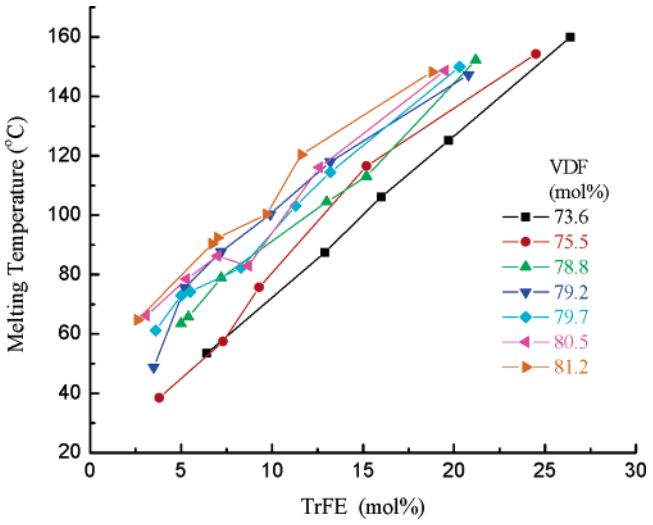

Figure 5. The melting temperature as a function of chemical composition of the terpolymer.

interpreted as an indication of uniform polymer crystalline morphology, owing to the random distributed CTFE and TrFE components generated by the reductive reaction. The melting and Curie temperatures are plotted against the terpolymer chemical compositions in Figures 5 and 6. It is shown that both melting and Curie temperatures increase with increasing TrFE content under certain VDF concentrations. These results agree quite well with the FTIR spectra showing all-trans conformation of the β-phase for high concentration of TrFE component in the polymers. Compared to the $tttg^+tttg^-$ conformation of the γ-phase, the β-phase possessing longer trans sequence in the polymer chains results in an increased activation energy barrier for phase transition and in turn high melting and Curie temperatures. For example, for the terpolymers containing 78.8 mol % VDF, as the TrFE concentration increases from 5 to 21 mol %, Curie transition and melting temperatures shift from 23 and 63 °C to about 98 and 152 °C, respectively, coinciding with the transformation of primary conformation from γ- to β-phases.

As a direct consequence of crystalline structure, the dielectric properties of the terpolymer appear to be strongly correlated to the chemical compositions. Figure 7 depicts the dependence of room-temperature dielectric constants on the terpolymer

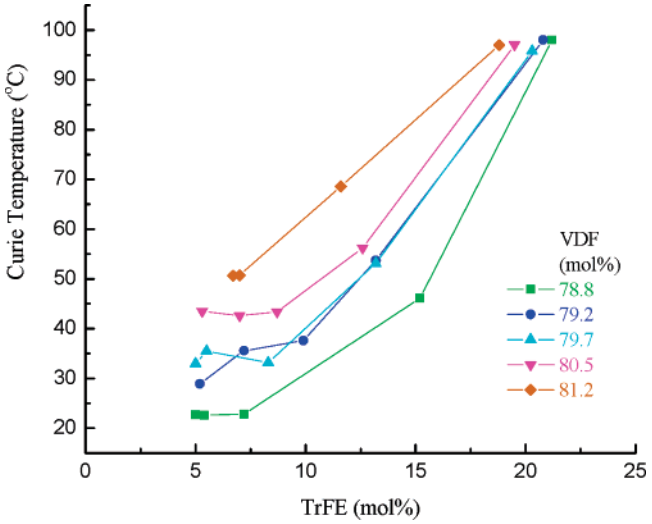

Figure 6. Curie transition tempearture vs chemical composition for the terpolymer.

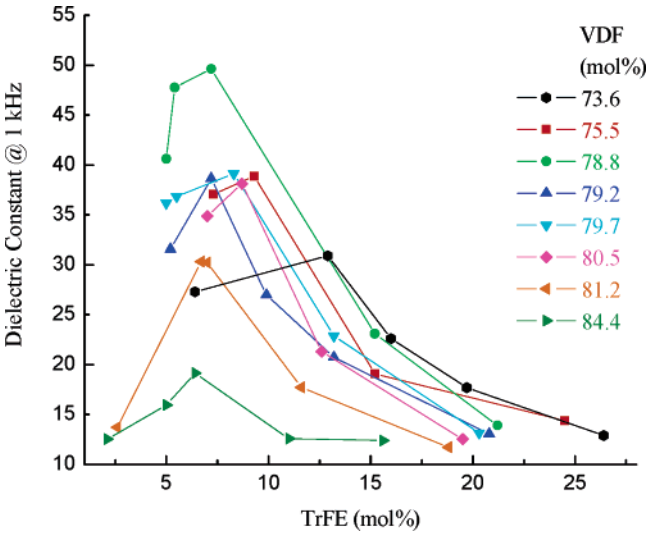

Figure 7. Composition dependence of room-temperature dielectric constant measured at 1 kHz.

compositions. Under a certain amount of VDF content, with decreasing TrFE concentrations in the terpolymers, the room-temperature dielectric constants correspondingly increase from 11 to 50 as a result of a gradual shift of Curie transition temperatures from about 100 °C to ambient temperature. Room-temperature dielectric constants larger than 40 (measured at 1 kHz) were achieved on the terpolymers containing 77−80 mol % VDF, 6−9 mol % TrFE, and 11−16 mol % CTFE. The highest room-temperature dielectric constant of about 50 at 1 kHz was revealed for the terpolymer having 78.8 mol % VDF, 7.2 mol % TrFE, and 14 mol % CTFE. This composition is quite different from the one prepared by direct terpolymerization, which shows a dielectric constant in the vicinity of 50 at a composition of 62 mol % VDF, 26 mol % TrFE, and 12 mol % CTFE.[13] For the polymers exhibiting the same dielectric constant, the one from the reductive reaction contains about 3−4 times less TrFE content than the terpolymers prepared via terpolymerization. This difference can be explained by the statement above, in which TrFE is present primarily as structural defects in the case of the terpolymer yielded from the reduction of P(VDF−CTFE)s, while TrFE exists as both head-to-tail normal and tail-to-tail defect sequences in the terpolymer from the direct terpolymerization process.

Conclusions

A new synthetic route to the ferroelectric polymers exhibiting high dielectric constants has been demonstrated in this work. The approach based on the quantitative dechlorination of P(VDF−CTFE) copolymers results in terpolymers with precisely controlled chemical compositions, thereby providing us an unprecedented opportunity to develop a library of the ferroelectric polymers for evaluating their structure−property relationships. As more TrFE is incorporated into the chain via increasing dechlorination ratios, crystallinity and thermal transition temperatures increase due to the conformation change from ferroelectric γ- to β-phases, leading to a shift of Curie transition temperatures from 23 to 102 °C and a variation of room-temperature dielectric constants from 50 to 11. Consequently, this method could be used to fine-tune the electroactive and thermal properties of the polymers to address the requirements of different applications. Compared with the polymer prepared via direct terpolymerization, the terpolymer synthesized by the dechlorination approach possesses a higher percentage of regiodefects at the same chemical composition, giving rise to a lower Curie transition temperature and thus a higher dielectric responses at ambient conditions.

Acknowledgment. This work was support by the National Science Foundation CAREER Award (DMR-0548146), Office of Naval Research (N00014-05-1-0455, N00014-05-1-0541), and the American Chemical Society Petroleum Research Fund (43042-G7).

Supporting Information Available: Tables of chemical composition, heat and temperature of melting and Curie transition, and dielectric constant for the ferroelectric fluoropolymers; ^{19}F NMR spectra and chemical shift assignments of the P(VDF−TrFE) copolymer and the terpolymer prepared via direct terpolymerization; and DSC profiles of the P(VDF−CTFE−TrFE) terpolymers. This material is available free of charge via the Internet at http://pubs.acs.org.

References and Notes

(1) Kawai, H. *Jpn. J. Appl. Phys.* **1969**, *8*, 975.
(2) Lovinger, A. J. *Science* **1983**, *220*, 1115.
(3) (a) Herbert, J. M., Glass, A. M., Wang, T. T., Eds. *The Application of Ferroelectric Polymers*; Chapman & Hall: New York, 1988. (b) Nalwa, H. S., Ed. *Ferroelectric Polymers*; Marcel Dekker: New York, 1995. (c) Bar-Cohen, Y., Ed. *Electroactive Polymer (EAP) Actuators as Artificial Muscles*, 2nd ed.; SPIE Press: Bellingham, 2004.
(4) (a) Higashihata, Y.; Sako, J.; Yagi, T. *Ferroelectrics* **1981**, *32*, 85. (b) Tajitsu, Y.; Chiba, A.; Furukawa, T.; Date, M.; Fukada, E. *Appl. Phys. Lett.* **1980**, *36*, 286.
(5) (a) Koga, K.; Ohigashi, H. *J. Appl. Phys.* **1986**, *59*, 2141. (b) Zhang, Q. M.; Zhao, J.; Shrout, T.; Kim, N.; Cross, L. E.; Amin, A.; Kulwicki, B. M. *J. Appl. Phys.* **1995**, *77*, 2549.
(6) Furukawa, T.; Date, M.; Fukada, E.; Tajitsu, Y.; Chiba, A. *Jpn. J. Appl. Phys.* **1980**, *19*, L109.
(7) (a) Davis, G. T.; Furukawa, T.; Lovinger, A. J.; Broadhurst, M. G. *Macromolecules*, **1982**, *15*, 329. (b) Yagi, T.; Tatamoto, M.; Sako, J. *Polym. J.* **1980**, *12*, 209. (c) Yamada, T.; Ueda, T.; Kitayama, T. *J. Appl. Phys.* **1981**, *52*, 948. (d) Furukawa, T.; Johnson, G. E.; Bair, H. E. *Ferroelectrics* **1981**, *32*, 61.
(8) (a) Zhang, Q. M.; Bharti, V.; Zhao, X. *Science* **1998**, *280*, 2102. (b) Lovinger, A. J. *Macromolecules* **1985**, *18*, 910. (c) Daudin, B.; Dubus, M. *J. Appl. Phys.* **1987**, *62*, 994.
(9) (a) Tashiro, K.; Nishimura, S.; Kobayashi, M. *Macromolecules* **1988**, *21*, 2463. (b) Furukawa, T.; Seo, N. *J. Appl. Phys.* **1990**, *29*, 675.
(10) (a) Casalini, R.; Roland, C. M. *Appl. Phys. Lett.* **2001**, *79*, 2627. (b) Gao, Q.; Scheinbeim, J. I. *Macromolecules* **2000**, *33*, 7564. (c) Casalini, R.; Roland, C. M. *J. Polym. Sci., Part B: Polym. Phys.* **2002**, *40*, 1975.
(11) (a) Yuki, T.; Ito, S.; Koda, T.; Ikeda, S. *J. Appl. Phys.* **1998**, *37*, 5372. (b) Ikeda, S.; Suzaki, H.; Nakami, S. *J. Appl. Phys.* **1992**, *31*, 1112.

(12) (a) Cheng, Z.; Olson, D.; Xu, H.; Xia, F.; Hundal, J. S.; Zhang, Q. M.; Bateman, F. B.; Kavarnos, G. J.; Ramotowski, T. *Macromolecules* **2002**, *35*, 664. (b) Bobnar, V.; Vodopivec, B.; Levstik, A.; Cheng, Z.; Zhang, Q. M. *Phys. Rev. B* **2003**, *67*, 094205/1.
(13) Xu, H.; Cheng, Z.; Olson, D.; Mai, T.; Zhang, Q. M.; Kavarnos, G. *Appl. Phys. Lett.* **2001**, *78*, 2360.
(14) Nalwa, H., Ed. *Handbook of Low and High Dielectric Constant Materials and Their Applications*; Academic Press: London, 1999.
(15) (a) Naber, R. C. G.; Tanase, C.; Blom, P. W. M.; Gelinck, G. H.; Marsman, A. W.; Touwslager, F. J.; Setayesh, S.; de Leeuw, D. M. *Nat. Mater.* **2005**, *4*, 243. (b) Schroeder, R.; Majewski, L. A.; Grell, M. *Adv. Mater.* **2005**, *17*, 1535. (c) Stadlober, B.; Zirkl, M.; Beutl, M.; Leising, G. *Appl. Phys. Lett.* **2005**, *86*, 242902. (d) Müller, K.; Paloumpa, I.; Henkel, K.; Schmeisser, D. *J. Appl. Phys.* **2005**, *98*, 056104.
(16) (a) Sakagami, T.; Arakawa, N.; Teramoto, Y.; Nakamura, K. U.S. Patent 4,554,335, 1985. (b) Inukai, H.; Kawai, N.; Kitahara, T.; Kai, S.; Kubo, M. U.S. Patent 5,087,679, 1992. (c) Chung, T. C.; Petchsuk, A. *Macromolecules* **2002**, *35*, 7678. (d) Honn, F. J.; Hoyt, J. M. U.S. Patent 3,053,818, 1962.
(17) Yagi, T.; Tatemoto, M. *Polym. J.* **1979**, *11*, 429.
(18) Lu, Y.; Claude, J.; Neese, B.; Zhang, Q. M.; Wang, Q. *J. Am. Chem. Soc.* **2006**, *128*, 8120.
(19) Moggi, G.; Bonardelli, P. *J. Polym. Sci. Polym. Phys.* **1984**, *22*, 357.
(20) Cais, R. E.; Kometani, J. M. *Macromolecules* **1985**, *18*, 1354.
(21) Murasheva, Y. M.; Shashkov, A. S.; Galil-Ogly, F. A. *Polym. Sci. U.S.S.R.* **1980**, *21*, 968.
(22) (a) Ferguson, R. C.; Brame, E. G., Jr. *J. Phys. Chem.* **1979**, *83*, 1397. (b) Tonelli, A. E.; Schilling, F. C.; Cais, R. E. *Macromolecules* **1982**, *15*, 849.
(23) (a) Reynolds, N. M.; Kim, K. J.; Chang, C.; Hsu, S. L. *Macromolecules* **1989**, *22*, 1092. (b) Kim, K. J.; Kim, G. B.; Valencia, C. L.; Rabolt, J. F. *J. Polym. Sci., Part B: Polym. Phys.* **1994**, *32*, 2435. (c) Osaki, S.; Ishida, Y. *J. Polym. Sci.* **1975**, *13*, 1071.
(24) (a) Klein, R. J.; Runt, J.; Zhang, Q. M. *Macromolecules* **2003**, *36*, 7220. (b) Klein, R. J.; Xia, J.; Zhang, Q. M.; Bauer, F. *J. Appl. Phys.* **2005**, *97*, 094105. (c) Bobnar, V.; Vodopivec, B.; Levstik, A.; Kosec, K. Hilczer, B.; Zhang, Q. M. *Macromolecules* **2003**, *36*, 4436.
(25) Furukawa, T. *Phase Transitions* **1989**, *18*, 143.
(26) (a) Sanchez, I. C.; Eby, R. K. *Macromolecules* **1975**, *8*, 638. (b) Lovinger, A. J.; Davis, G. T.; Furukawa, T.; Broadhurst, M. G. *Macromolecules* **1982**, *15*, 323. (c) Lovinger, A. J.; Furukawa, T.; Davis, G. T.; Broadhurst, M. G. *Polymer* **1983**, *24*, 1225.
(27) Warren, B. E. *X-ray Diffraction*; Dover Publications: New York, 1990.

MA061311I